

# Investigation of orientation transitions and coexistence of magnetic phases in the cubic ferrimagnet GdIG

N. F. Kharchenko, V. V. Eremenko, and S. L. Gnatchenko

*Physico-technical Institute of Low Temperatures, Ukrainian Academy of Sciences*

(Submitted April 25, 1975)

*Zh. Eksp. Teor. Fiz.* **69**, 1697–1709 (November 1975)

Sublattice fracture induced in the cubic ferrimagnet GdIG by a magnetic field is investigated visually in polarized light and by measuring the Faraday rotation of the polarization plane in small parts of the sample. The investigations are performed near the magnetic compensation temperature of the ferrite for two orientations of the magnetic field: along the axes of easy [111] and difficult [100] magnetization. Variation of the temperature at a constant magnetic field revealed coexisting magnetic phases in the vicinity of first-order phase transitions between the collinear and canted structures ( $\mathbf{H} \parallel [111]$ ) and also between low- and high-temperature noncollinear structures ( $\mathbf{H} \parallel [111]$  and  $\mathbf{H} \parallel [100]$ ). For both cases of field orientation the regions of existence of the magnetic phases in GdIG are plotted in the  $(M, T)$  plane. The experimental results are compared with the results of calculations carried out in the molecular-field approximation with allowance for the cubic symmetry and the three-sublattice magnetic structure of the gadolinium iron garnet.

PACS numbers: 75.50.Gg, 78.20.Ls

Transitions of a ferrimagnet from the collinear to the skewed state, induced by an external magnetic field (see [1], where references to earlier work can be found) can be regarded as orientational transitions of the second kind only in the isotropic case. In real ferrites, as a result of the action of magnetic crystallographic anisotropy, the continuity of the motion of the magnetic moments of the sublattices during the process of their fracture may become violated. In the rare-earth iron garnets, which are easy to investigate, transitions that are smooth in the isotropic approximation, from the collinear states to canted states, become at certain orientations and magnetic-field values first-order transitions, and new phase transitions appear between the noncollinear structures. [2-4] Near the magnetic-compensation temperature, the stability regions of different magnetic phases overlap. The small energy difference between the phases and the presence in the crystal of lattice and other inhomogeneities can lead to coexistence, in a certain temperature region, of stable and metastable states. Moreover, even in a perfect crystal the interphase boundary may turn out to be thermodynamically favored, owing to the increase of the entropy on account of the ambiguity in the position of the boundary in the absence of demagnetizing fields. [5] Furthermore, in the case of crystals having several easy-magnetization directions and symmetrical orientation of the magnetic field, energywise equivalent magnetic twins can be formed in the course of the sublattice fracture, with identical magnetic structure (with identical kink angles of the magnetic sublattices, but with different azimuths).

By virtue of these circumstances, one cannot expect a homogeneous noncollinear magnetic structure of iron garnets with cubic magnetic anisotropy. Indirect [6-9] and direct visual [10-12] observations of rare-earth iron garnets show that the induced skewed magnetic structures are inhomogeneous even in a magnetic field of several dozen kOe. This makes it difficult to study the magnetic phase diagrams of cubic ferrimagnets, so that to determine the phase boundaries experimentally it is necessary to resort to methods that are sensitive to the directions of the magnetic moments of the individual sublattices. Magneto-optical methods, particularly visual-observation methods, are convenient for this purpose. We report here magneto-optical investigations, with

simultaneous visual observation, of the magnetic states of gadolinium iron garnet near its compensation temperature in weak magnetic fields  $H \lesssim (H_A H_{\text{exch}})^{1/2}$ . The results of the experiments are compared with calculations performed within the framework of the molecular field approximation with allowance for the three-sublattice structure of the GdIG.

## EXPERIMENTAL PROCEDURE

The magneto-optical activities of individual sublattices of rare-earth iron garnets differ appreciably. In gadolinium iron garnet in the visible part of the spectrum, the contribution of the gadolinium sublattice is negligible, and the contribution of the octahedral iron sublattice prevails over the contribution of the tetrahedral one. This makes it possible to determine readily, by measuring the magneto-optical activity, the angle between the light propagation direction and the magnetic-moment vector of the octahedral sublattice, and to distinguish visually between sample sections having different magnetic-sublattice rotation angles.

We used a longitudinal experimental geometry, wherein the magnetic field was parallel to the light propagation vector,  $\mathbf{H} \parallel \mathbf{k}$ . This geometry makes the magnetic twins, which differ only in the azimuthal angles of the magnetic moments of the sublattices but have identical projections of the sublattice moments on the  $H$  direction, invisible in observations based on the Faraday rotation of the polarization plane. The task of constructing the regions of the existence of magnetic phases is then greatly facilitated. A transverse geometry is convenient for the observation of magnetic twins. [10]

The usual optical scheme for the observation of magnetic domains in transparent crystals was supplemented by a recording setup. A mirror-diaphragm was placed in the image plane of the objective, and its dimensions corresponded to a sample region of approximately  $75 \mu$  diameter. The light that was not passed by the diaphragm was reflected from the mirror, passed through the analyzer, and entered an ocular that could be used to monitor visually, simultaneously with the measurements, the position of the diaphragm relative to the domain image. The registration setup incorporated an analyzer

executing harmonic oscillations of frequency  $\omega$  and crossed with a polarizer. The intensity of the light emerging from the analyzer, at low values of the analyzer azimuth modulation amplitude  $\gamma$  and of the Faraday rotation angle  $\Phi$ , is equal to

$$I = I_0(2\gamma\Phi \sin \omega t - 1/2\gamma^2 \cos 2\omega t + \Phi^2 + 1/2\gamma^2).$$

The signal of frequency  $\omega$  separated with the aid of a narrow-band amplifier and a synchronous detector is proportional to the rotation of the polarization plane of the light. The proportionality coefficient  $2I_0\gamma$  was determined with a Faraday compensator. Control measurements were also made with a compensator and a null circuit. The light source was an incandescent lamp. To prevent heating of the sample by the light, and to prevent radial temperature gradients, the thickness of the thermal filter was chosen such that further increase of the thickness had no effect on the domain configuration in all the investigated temperature and magnetic-field intervals.

The GdIG samples were cut in the form of plates oriented by x-ray diffraction in the (100) and (111) planes. After mechanical polishing, the plate thickness ranged from 30 to 50  $\mu$ . Some samples were subjected to additional chemical polishing, as well as to annealing in air or in an atmosphere of oxygen at 1000–1100°C. During the time of the investigation the sample was freely placed between two washers in a copper capsule. The capsule with the sample were placed in a cell filled with the heat-exchange gas or inside a bulky cold finger in vacuum. The sample temperature could be maintained constant within  $\pm 0.01^\circ\text{K}$ , or varied smoothly from 200 to 350°K at a rate from  $10^{-3}$  °K/sec to  $10^{-2}$  °K/sec. The temperature was measured with copper-constantan thermocouples. The absolute measurement error was estimated by us at about  $\pm 0.2^\circ\text{K}$ . The temperature gradient at the sample was monitored in various ways and did not exceed  $0.01^\circ\text{K/mm}$  for samples whose investigated part measured 1.5–2 mm.

The samples at our disposal sometimes contained blocks that became clearly pronounced near the compensation temperature when observed in a magnetic field. The blocks had different temperatures  $T_c$ . The maximum difference between the  $T_c$  amounted to several tenths of a degree. The results that follow pertain to either single-block samples or to an individual block of a sample.

## EXPERIMENTAL RESULTS

The visual observations have shown that the process of the transition of the gadolinium iron garnet from the collinear to the canted state is qualitatively different when the magnetic field is parallel to the easy and difficult magnetization axes [111] and [100] respectively. In the former case the canted phase appears in the form of individual growing regions, and in the latter there is a smooth uniform transition from the collinear to the canted state. Abrupt orientational transitions between the different noncollinear structures were observed in both cases.

a)  $H \parallel [111]$ . As the sample temperature approached the magnetic-compensation temperature  $T_c$ , clearly outlined sections appear in it, with optical density, at fixed polarizer positions, different from the density of the main part of the crystal. With further approach to  $T_c$  and then with increasing difference from it, new regions with different optical densities appear and replace one

another. By varying the position of the analyzer and measuring the Faraday rotation in individual domains, it is possible to distinguish and identify four domain types. Figure 1 illustrates the successive alternation of the magnetic states of the sample with changing temperature: the low temperature collinear state (grey sections) gives way to high-temperature canted state (dark sections), after which domains in the high-temperature canted state (new grey regions) appear and are replaced in turn by high-temperature collinear states (light sections). The contrast between the neighboring domains changes little with temperature, but decreases noticeably when the field intensity is increased. In fields of intensity higher than 9 kOe, it was possible to observe simultaneously only two types of domain. After one state is replaced by another, the sample becomes homogeneous, after which the next alternation of states takes place. Figure 2 shows the growth of the high-temperature canted phase (lighter sections) at a magnetic-field intensity 14 kOe.

In weak fields the walls between the domains are frequently localized near scratches and other surface defects. In strong fields, surface defects do not influence the arrangement of the walls (Figs. 1 and 2). The walls are frequently not perpendicular to the sample surface, and regions with different states are frequently projected on one another in the course of observation. Nonetheless, by tracing the positions of the phase boundaries it is possible to determine reliably the instants when domains of various types appear and vanish also in weak fields.

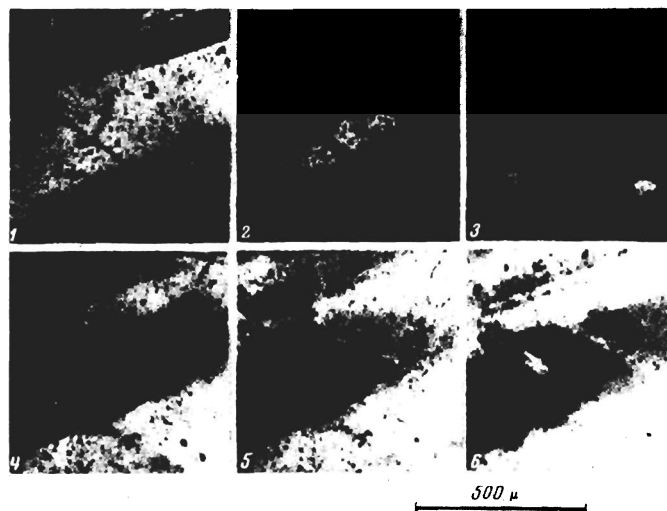


FIG. 1. Domain structure produced upon reorientation of the magnetic moments of the GdIG sublattices at  $H \parallel [111]$ ,  $H = 6$  kOe: 1–284.3, 2–284.7, 3–284.8, 4–285.2, 5–285.4, 6–285.6 K.

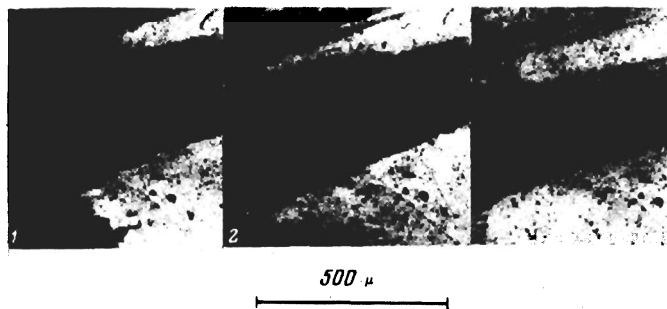


FIG. 2. The same as in Fig. 1, but at  $H = 14$  kOe.

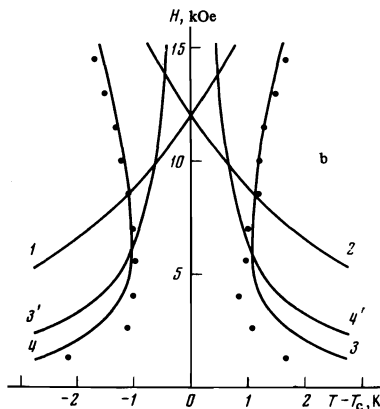
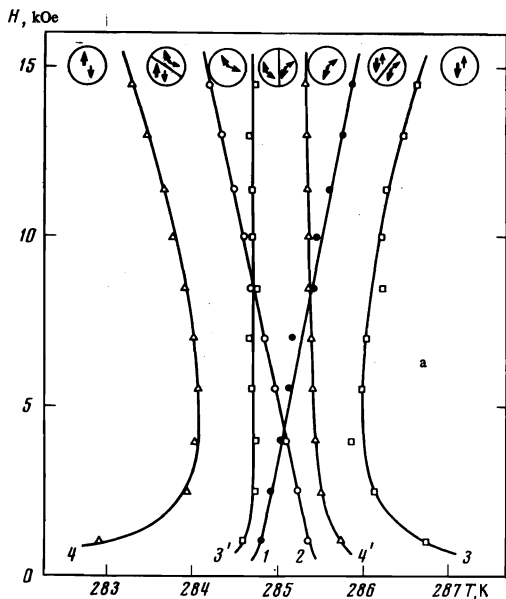


FIG. 3. Diagram of magnetic states of GdIG at  $H \parallel [111]$ : a—experimentally obtained boundaries of the existence of magnetic phases, b—phase-stability-loss lines calculated with the aid of formula (3). Points—experimental. The numbers at the curves denote the boundaries of the corresponding phases: 1 and 2—high- and low-temperature collinear, 3, 3' and 4, 4'—high- and low-temperature canted.

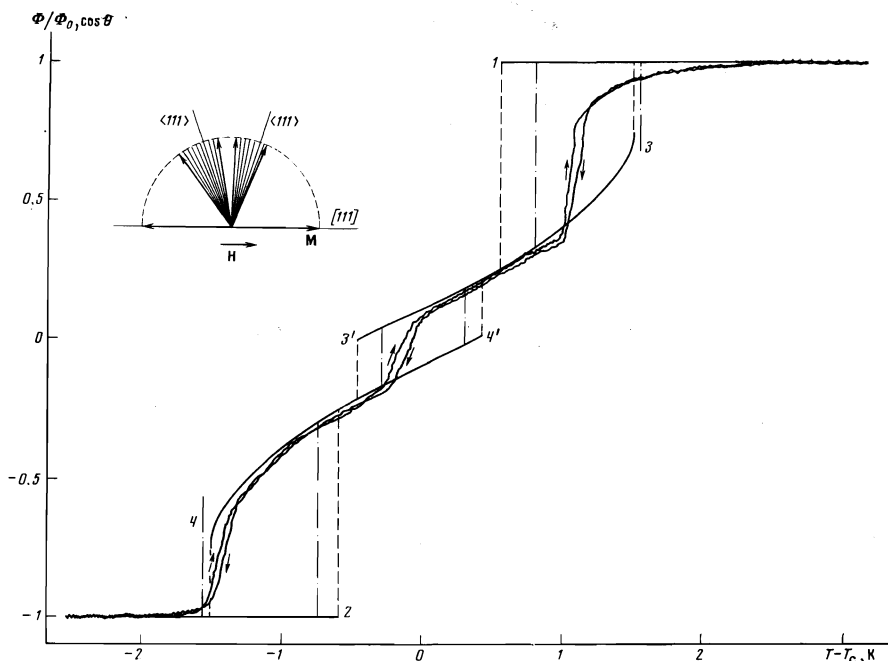


FIG. 4. Rotation of sublattices in GdIG at a fixed magnetic field of 14 kOe parallel to  $[111]$ , and at variable temperature; the curves with noise show the experimental dependence of the Faraday rotation by a sample section of  $75 \mu$  diameter, solid lines—calculated dependence of the rotation angle, dashed lines—regions of metastable states, dash-dot lines—temperature intervals in which the coexistence of magnetic phases was observed.

The sample magnetic-state diagram obtained with the aid of visual observations is shown in Fig. 3a.

The sublattice rotation angle in the coexisting phases could be determined by measuring the Faraday rotation in a magnetically-homogeneous section of the sample, using a diaphragm placed in the plane of the magnified image of the crystal. By moving the diaphragm over the image of the sample or by shifting the domain walls by slightly changing the temperature, it was possible to determine the law governing the variation of the Faraday rotation and the angle of rotation of the sublattices in the canted phases with changing temperature or field. Figure 4 shows the characteristic changes of the Faraday rotation by a section of the sample of  $75 \mu$  diameter at variable temperature and fixed magnetic field. The steep sections correspond to passage through the working region of the sample of the domain walls and to replacement of one state by another. Knowing the spontaneous rotation  $\Phi_0$  at  $M_1 \parallel k$ , determined in the collinear state of the GdIG, we can find the cosine of the angle of rotation of the magnetic moment of the active sublattice and construct the diagram of its motion (Fig. 4).

b)  $H \parallel [100]$ . When observation is through crossed polarizers, the appearance of the domains is preceded by a homogeneous bleaching of the sample as its temperature approaches  $T_C$ ; this bleaching corresponds to a smooth turning of the sublattices. In a temperature interval of approximate width  $1^\circ K$  near  $T_C$ , the sample ceases to be magnetically uniform. It breaks up into domains of two types, having different signs and values of the Faraday rotation. Figures 5 and 6 demonstrate the character of the appearance and growth of the new phase with increasing temperature. The motion of the walls in fields weaker than 10 kOe is frequently jumplike. The irreversibility of the wall motion manifests itself particularly strongly at low field intensities (up to 5–6 kOe), when the walls are localized near surface defects. In fields stronger than 9–10 kOe, the surface defects have a smaller influence on the wall position, and the form of the domains changes appreciably (Fig. 6).

When plotting the phase diagram (Fig. 7), the region where the low- and high-temperature noncollinear phases

coexist was determined visually, and the walls separating the regions of the canted and collinear states were revealed by the start of the turning of the sublattices. The temperature at which the noncollinear phase appears in a given field was taken to be the temperature at which the sample decreases the Faraday rotation angle by an amount comparable with the noise (Fig. 8). Figure 8

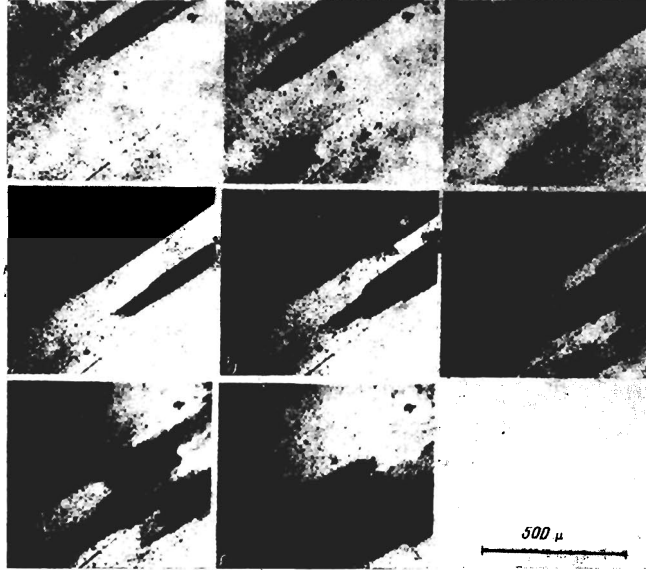


FIG. 5. Domain structure produced upon reorientation of the magnetic moments of the GdIG sublattices at  $H \parallel [100]$ ,  $H = 7$  kOe; 1—284.75, 2—284.86, 3—284.91, 4—284.98, 5—285.07, 6—285.16, 7—285.25, 8—285.33 K.

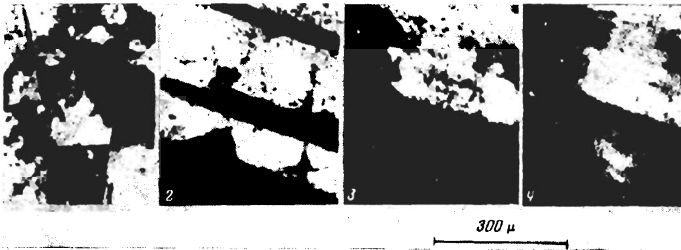


FIG. 6. The same as in Fig. 5, but for a sample with many surface defects. Temperature constant at  $T = 284.9^\circ\text{K}$ ; 1— $H = 0.2$ , 2—5.8, 3—10.2, 4—13.3 kOe.

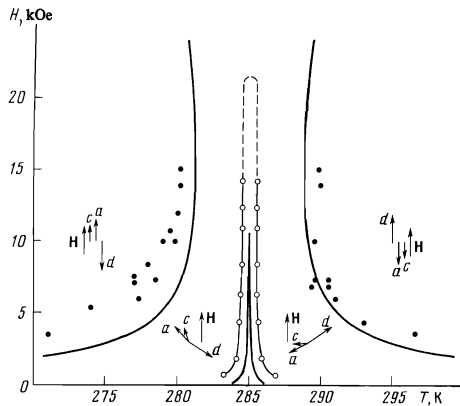


FIG. 7. Diagram of magnetic states of GdIG at  $H \parallel [100]$ ; the solid lines show the calculated phase boundaries and the region of metastable states; ●—experimental points of transition of ferrite from collinear to canted states; the light circles and the thin lines delineate the observed region of existence of magnetic inhomogeneities; dashed—result of linear extrapolation of the  $\Delta\Phi(H)/2\Phi_0$  plot of Fig. 9.

shows the variation of the rotation with temperature in a small sample section that is in a homogeneous state. The central part of the curve, corresponding to the inhomogeneous state of the measured section, is not shown. During the time that the interphase walls pass through the small sample region of  $75 \mu$  diameter, the sample temperature remains practically unchanged and the difference between the Faraday rotation angles of the polarization plane at the instants of appearance of the new magnetic state  $\Phi_1$  and the vanishing of the old one  $\Phi_2$  gives the difference between the cosines of the sublattice rotation angles in the coexisting phases. Figure 9 shows a plot of  $(\Phi_1 - \Phi_2)/2\Phi_0$  against the magnetic field intensity.

## DISCUSSION

The process of sublattice fracture in a three-sublattice cubic ferrimagnet was discussed by us in [9], and we shall use those results to construct the lability lines of the GdIG magnetic phases. We denote by  $\theta_i$  (Fig. 10) the angle of rotation of the magnetic moment of the  $i$ -th sublattice from its direction in the initial collinear configuration at a given temperature. The index  $i = 1, 2, 3$ , denotes respectively the d, a, and c sublattices,  $\theta = (1/2)(\theta_1 + \theta_2)$  is the average angle of rotation of the iron sublattices. The angles  $\theta_1, \theta_2$ , and  $\theta$  are close to each other, inasmuch as at the employed field intensities we have

$$\theta_1 - \theta_2 = \frac{\lambda_{23}\sigma_2^2 - \lambda_{13}\sigma_1^2}{2\sigma_1\sigma_2\lambda_{12}} h \sin \theta \leq 0.2^\circ.$$

Here  $\sigma_i = M_i \cos n_i \pi$  (where  $n_i = 0$  or  $1$ ) are the projections of the magnetic moments of the sublattices in the initial collinear configuration on the direction of the field  $H$ , and  $h = H/\lambda(\sigma_1 + \sigma_2)$ . For the lines of the extremal values of the skewed-phase energy, characterized by an iron-sublattice rotation angle  $\theta$ , we can write down the approximate expression

$$\left(1 + \frac{\lambda}{\lambda_{12}} + \frac{\lambda_{13} + \lambda_{23}}{\lambda_{12}} \frac{\sigma_3}{\sigma_1 + \sigma_2}\right) h^2 \cos \theta + \left(1 + \frac{\lambda_{13}\lambda_{23}}{\lambda\lambda_{12}} \frac{\sigma_3}{\sigma_1 + \sigma_2}\right) \left(1 + \frac{\sigma_3}{\sigma_1 + \sigma_2}\right) h + \left(1 + \frac{\lambda_{13}\lambda_{23}}{\lambda\lambda_{12}} \frac{\sigma_3}{\sigma_1 + \sigma_2}\right) \kappa \frac{1}{\sin \theta} \frac{\partial f(\theta, \varphi_0)}{\partial \theta} = 0, \quad (1)$$

which is valid for low external magnetic-field intensities  $|h| \ll 1$ . Here  $\kappa = K/\lambda(\sigma_1 + \sigma_2)^2$ ,  $K$  is the anisotropy constant, and the azimuthal angle  $\varphi$  in the expression for the angular dependence of the anisotropy energy  $f(\theta, \varphi)$  is taken equal to the azimuthal angle of one of the light planes of the (110) type. The magnetizations of the iron sublattices  $\sigma_1$  and  $\sigma_2$  in a small temperature interval in the vicinity of  $T_C$  can be regarded as independent of the temperature and of the magnetic field, and the Brillouin function in the expression for the magnetization of the rare-earth sublattice can be expanded in a series in which we need retain only the terms linear in  $h$  and  $t = (T - T_C)/T_C$ :

$$M_s = M_{sc} + M_{sc}'(h \cos \theta + t), \quad M_{sc} = M_s(T = T_C, H = 0), \quad M_{sc}' = M_{s0} \left( \frac{\partial B_s(x)}{\partial x} \right)_{T=T_C, H=0} \quad (2)$$

For the equilibrium values of the rotation angle  $\theta$  for given  $h$  and  $t$  we then obtain the equations

$$H \parallel [111], \quad h^2 \alpha \cos \theta + h t m_s' \beta + \kappa \beta \frac{1}{\sin \theta} \frac{\partial f}{\partial \theta} = 0, \quad \frac{1}{\sin \theta} \frac{\partial f}{\partial \theta} = -\frac{4}{3} \cos \theta + \frac{7}{3} \sin^2 \theta \cos \theta - \frac{\sqrt{2}}{3} (4 \sin^3 \theta - 3 \sin \theta); \quad (3a)$$

$$H \parallel [100], \quad \cos^3 \theta - \frac{1}{3} \left(1 - \frac{h^2 \alpha}{\kappa \beta}\right) \cos \theta + \frac{m_s'}{3\kappa} h t = 0, \quad \alpha = 1 - m_s' \beta + \frac{\lambda - \lambda_{13} - \lambda_{23}}{\lambda_{12}}, \quad \beta = 1 - \frac{\lambda_{13}\lambda_{23}}{\lambda\lambda_{12}}, \quad m_s' = \frac{M_{sc}'}{M_1 - M_2} \quad (3b)$$

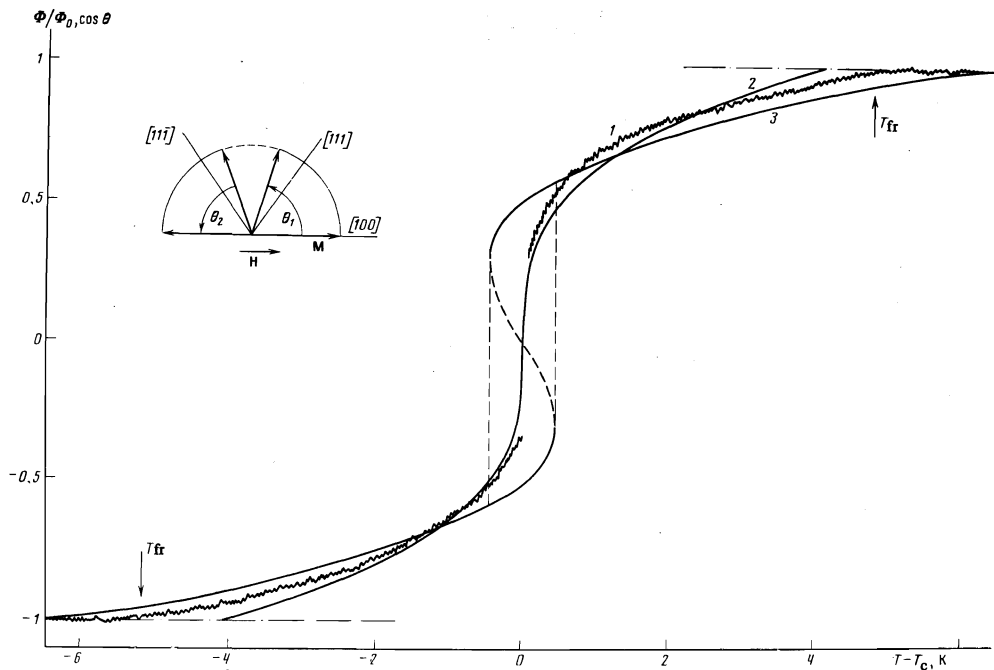


FIG. 8. Rotation of sublattices in GdIG at a fixed magnetic field  $H \parallel [100]$  and at a variable temperature: 1—experimental plot of  $\Phi(T)$  at  $H = 10.5$  kOe, corresponding to a homogeneous sample; 2, 3—calculated dependence of the cosine of the rotation angle of the sublattices at  $H_C = 10.5$  kOe (2) and  $H_C = 21.5$  kOe (3). A better agreement between the experimental and calculated curves is observed at  $H_C = -\lambda(M_1 - M_2)(\kappa\beta/\alpha)^{1/2} = 10.5$  kOe.

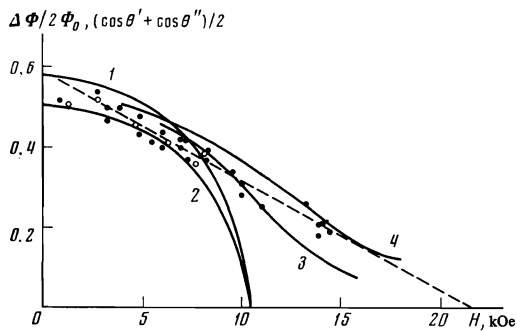


FIG. 9. Faraday rotation and of the sublattice rotation angles in homogeneous states of the GdIG that are closest to  $T_C$  as functions of the magnetic field intensity. Points:  $\bullet$ —experimental values of the difference  $(\Phi_1 - \Phi_2)/2\Phi_0$  for annealed samples,  $\circ$ —the same for annealed and chemically polished samples; 1, 2—calculated plots of the differences of the cosines of the sublattice rotation angle in the coexisting phases; 3, 4—plots of the cosine of the sublattice rotation angle at  $T = T_C + \Delta T'$  ( $3 - \Delta T' = 0.1$  K,  $4 - \Delta T' = 0.2$  K).

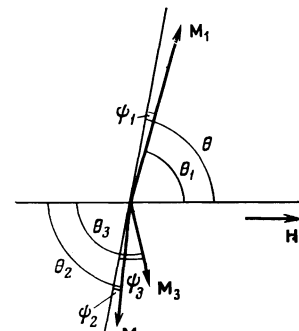


FIG. 10

Taking into account the requirements of the energy minimum for stable states, we can construct with the aid of (3) the stability lines of the skewed phases. The results of the calculations are shown in Figs. 3b and 7. In the calculations we used the following values of the sublattice magnetic moments<sup>[13,14]</sup>:  $M_1 = 75.5$  cgs emu-g<sup>-1</sup>,  $M_2 = 53.3$  cgs emu-g<sup>-1</sup>,  $M_{30} = 124.4$  cgs emu-g<sup>-1</sup>. The ratio  $\beta/\alpha$  was taken equal to 8.9 from<sup>[9]</sup>, where it was determined from the slope of the boundaries between the skewed and collinear phases of the GdIG in stronger fields. The constant is magnetic anisotropy  $K = -6.7 \times 10^3$  erg/cm<sup>3</sup> =  $-1.04$  erg/g<sup>[15]</sup>, and the effective exchange constant  $\lambda = 11\,550$  Oe-g/cgs emu was determined from the value  $T_C = 285.0^\circ$  K. The exchange field acting on the rare-earth sublattice is equal to  $-\lambda(M_1 - M_2) = 2.56 \times 10^5$  Oe, and the reduced anisotropy constant is  $\kappa = 1.85 \times 10^{-4}$ .

Figure 3b shows the calculated stability-loss lines of the collinear high-temperature and low-temperature (2) phases, and also of both skewed phases [high-temperature (3, 3') and low-temperature (4, 4')] in the case

$H \parallel [111]$ . The figure shows also the experimental points that bound the region inside which the skewed phases were observed. Comparison of Figs. 3a and 3b shows that the results of the calculations agree with experiment, namely, the regions of phase coexistence lie inside the corresponding regions of the metastable states. In Fig. 4 are compared the experimental and calculated temperature dependences of the angle of rotation of the iron sublattices at a fixed magnetic field intensity  $H = 14$  kOe having the same orientation. The dashed lines show the temperature limits of the metastable states, and the dash-dot lines show the observed phase-coexistence limits. Good agreement between the experimental and calculated curves is observed in fields  $H > 10$  kOe. At lower field intensities, the central jump of the rotation is smaller than the calculated one. Its decrease is apparently due to the overlap of domains of different phases in weak fields.

In the case  $H \parallel [100]$  the equation for the second-order phase transition phase lines, which delineate the regions of the collinear and skewed states, can be obtained from (3b) by substituting the value  $\cos \theta = 1$ :

$$t_{fr} = -(2\kappa/m_s' h + \kappa\alpha/m_s' \beta). \quad (4)$$

The obtained curves are compared with the experimental points in Fig. 7. Taking into account the approximate

character of the method used to determine the temperature  $T_{fr}$  of the transition to the skewed state, the agreement between the calculation and experiment should be regarded as good. The figure shows also the calculated boundaries of the region of metastable noncollinear states, which are determined from the requirement that the solution of Eq. (3b) be ambiguous:

$$t_{met} = -\frac{2\kappa}{9m_s h} \left(1 - \frac{h^2}{h_c^2}\right)^{1/2}, \quad (5)$$

where the critical field is  $h_c = (\kappa\beta/\alpha)^{1/2}$ . The here-presented experimentally observed region of existence of magnetic inhomogeneities (the dashed section corresponds to extrapolation of the plot of  $\Delta\Phi/2\Phi_0$  shown in Fig. 9) greatly exceeds the calculated region of metastable states. Let us examine this singularity in greater detail.

It must be noted first that the observed coexistence of different magnetic phases cannot be due to the demagnetization fields, since the jumps of the magnetization occurring during the orientational transitions in GdIG do not exceed, at best, several gauss, and the domain-structure period due to the action of the demagnetization fields should exceed the dimensions of the sample. In addition, the temperature interval of the existence of the domain structure, if this is the mechanism producing the structure, should not exceed  $4\pi\Delta M(dH_{tr}/dT)^{-1} < 10^{-2}$  K. If we disregard chemical and stoichiometric inhomogeneities, then the causes of the magnetic stratification of the sample should be analogous to those leading to the appearance of a domain structure in antiferromagnets.<sup>[5]</sup> In particular, the domain wall may turn out to be energetically more favored in a real sample with lattice defects, owing to the lowering of the elastic energy of the crystal at the place where the wall is localized, owing to the magnetoelastic interaction. Walls of this kind can stabilize the inhomogeneous state of the sample with sections of the thermodynamically stable and metastable phases. The realization of the metastable states is evidenced by the localization of the domain walls on the surface defects (Figs. 1 and 7), by the irreversibility of the wall motion, and by the position of the temperature "window" in which the canted phases exist at  $H \parallel [111]$ . If the inhomogeneous magnetic state were due only to inhomogeneity of the compensation temperature over the sample, then the lowest width of the temperature band, inside which the sample is inhomogeneous, would be observed in a zero magnetic field. Actually the width of the band is minimal in a field of about 5 kOe, in accord with the position of the "window" of the metastable states (Fig. 3b). The proximity of the experimental points to the boundaries of the metastable canted phases indicates that there is a small difference between the energies of the thermodynamically-stable collinear and metastable skewed states. The fact that the region of coexistence of the high- and low-temperature skewed phases exceeds the region of the metastable states at  $H \parallel [100]$  may be due to the inhomogeneity of the compensation temperature over the sample. No unified front separating the two states was observed in the investigated samples, and furthermore the domains were significantly different in form at low and high field intensities. It can therefore be concluded that the sections of the sample with different values of  $T_c$  have microscopic dimensions. Taking into account the need for increasing the energy when the domain wall is produced, we can explain the decrease of the dimensions of the domains with increasing field intensity. When the field is increased, the positive energy

of the boundary decreases, since the angle of rotation of the magnetic moments in the boundary decreases. We can estimate the dependence of the sublattice rotation angle at the instant of appearance of the inhomogeneities on the magnetic field intensity by recognizing that the inhomogeneities are observed near  $T_c$ , starting with the temperature  $T'$ .

Figure 9 shows plots of  $(\cos \theta)_{T=T'}$  against  $H$  at values of the difference  $|T' - T_c|$  equal to 0.1 and 0.2°K and close to the experimental ones in the investigated small sections of the sample. The figure shows also plots of the difference of the cosines of the sublattice turning angles in the coexisting equilibrium phases (1)

$$\frac{1}{2}(\cos \theta' + \cos \theta'') = \frac{1}{\sqrt{3}} \left(1 - \frac{h^2}{h_c^2}\right)^{1/2}$$

and between the metastable and stable phases (2) farthest from  $T_c$ :

$$\frac{1}{2}(\cos \theta' + \cos \theta'') = \frac{1}{3} \left(1 - \frac{h^2}{h_c^2}\right)^{1/2}.$$

It is seen from Fig. 9 that the disparity between the experimental points and curve 1 (or 2) in the field region  $H > H_c = 10.5$  kOe can be attributed to the inhomogeneity of  $T_c$  over the volume of the sample. We note that the change of  $T_c$  in small sections of the crystal can be due to lattice defects and associated microstresses. For rough estimates we can use the results of<sup>[16]</sup>. According to<sup>[16]</sup>, to shift  $T_c$  of GdIG by 0.2°K it is necessary to apply a hydrostatic pressure

$$\Delta T_c(dT_c/dP)^{-1} = 0.2 \cdot (0.95 \cdot 10^{-3} \text{ K/bar})^{-1} \approx 2 \text{ kgf/mm}^2$$

which can be realized in the crystal. In connection with the latter, it remains unclear why the surface defects, near which the stresses are particularly large, do not manifest themselves in strong fields. Annealing of the sample and chemical polishing of its surface did not influence noticeably the width of the region of the coexistence and the behavior of GdIG in the field  $H > H_c$ .

Nor is it excluded that the behavior of GdIG near  $T_c$  in fields  $H \gtrsim H_c$  can be explained by taking into consideration the entropy of the interphase boundaries, the positions of which are not fixed by the demagnetizing fields and can shift by an amount equal to several lattice constants, without changing the energy of the system. The estimates made in<sup>[6]</sup> show that the domain walls in antiferromagnets may, at sufficiently high temperatures, turn out to be thermodynamically favored, because of the entropy contribution to the free energy of the wall. An increase of the entropy in an inhomogeneous state can influence both the width of the region of the phase coexistence (more accurately, it can lead to a new, mixed state) and the position of the critical point ( $T_c H_c$ ). The value of the entropy contribution should become enhanced by the circumstance that the considered critical point is an eightfold critical point.

Summarizing, we can state that rotation of the sublattices in gadolinium iron garnet during the course of the sublattice fracture can be described satisfactorily by molecular field theory with allowance for the cubic magnetic anisotropy and the three-sublattice structure of the iron garnets. There is no unambiguous explanation for the behavior of GdIG near the critical point. It is of interest to clarify the role of the entropy of the interphase boundaries in magnetic orientational transitions, particularly for critical transitions in cubic ferrimagnets.

In conclusion, we take the opportunity to thank O. M. Kononov, M. B. Kosmyn, and V. M. Puzikov for supplying the GdIG samples.

- <sup>1</sup>K. P. Belov, Ferrity v sil'nykh magnitnykh polyakh (Ferrites in strong magnetic fields), Nauka, 1972, pp. 63—92.
- <sup>2</sup>B. P. Goranskii and A. K. Zvezdin, Pis'ma Zh. Eksp. Teor. Fiz. **10**, 196 (1969) [JETP Lett. **10**, 124 (1969)].
- <sup>3</sup>R. Alben, Phys. Rev. Lett. **24**, 68 (1970); Phys. Rev. **2B**, 2767 (1970).
- <sup>4</sup>A. K. Zvezdin and V. M. Matgeev, Zh. Eksp. Teor. Fiz. **62**, 260 (1971) [Sov. Phys.-JETP **35**, 140 (1971)].
- <sup>5</sup>M. M. Fartztdinov, Usp. Fiz. Nauk **84**, 611 (1964) [Sov. Phys.-Usp. **7**, 855 (1965)].
- <sup>6</sup>H. F. Kharchenko, V. V. Eremenko, and L. I. Belyi, Zh. Eksp. Teor. Fiz. **55**, 419 (1968) [Sov. Phys.-JETP **28**, 219 (1969)].
- <sup>7</sup>O. A. Grzhegorzhevskii and R. V. Pisarev, Zh. Eksp. Teor. Fiz. **65**, 633 (1973) [Sov. Phys.-JETP **38**, 312 (1974)].
- <sup>8</sup>E. V. Matyushkin and V. N. Venitskii in: Fizika kond. sost (Phys. of Cond. State) FTINT Akad. Nauk Ukr. SSSR **30**, 129 (1974).
- <sup>9</sup>N. F. Kharchenko, V. V. Eremenko, S. L. Gnatchenko, L. I. Belyi, and E. M. Kabanova, Zh. Eksp. Teor. Fiz. **68**, 1073 (1975) [Sov. Phys.-JETP **41**, 531 (1975)].
- <sup>10</sup>V. V. Eremenko, N. F. Kharchenko, and S. L. Gnatchenko, Digests of the Intermag. Conference, 1974, Toronto, Canada, 7-7.
- <sup>11</sup>F. V. Lisovskiĭ and V. I. Shapovalov, Pis'ma Zh. Eksp. Teor. Fiz. **20**, 128 (1974) [JETP Lett. **20**, 55 (1974)].
- <sup>12</sup>N. F. Kharchenko, V. V. Eremenko, and S. L. Gnatchenko, Pis'ma Zh. Eksp. Teor. Fiz. **20**, 612 (1974) [JETP Lett. **20**, 280 (1974)].
- <sup>13</sup>J. D. Lister and G. B. Benedek, J. Appl. Phys. **37**, 1330 (1966).
- <sup>14</sup>E. E. Anderson, Phys. Rev. **134**, A1581 (1964).
- <sup>15</sup>G. P. Podrigue, H. Meyer, and R. V. Jones, J. Appl. Phys. **31**, 3765 (1960).
- <sup>16</sup>D. Bloch, F. Chaisse, and R. Pauthenet, J. Appl. Phys. **38**, 1029 (1967).

Translated by J. G. Adashko  
182